nature genetics

Overexpression of *Fto* leads to increased food intake and results in obesity

Chris Church[1], Lee Moir[1], Fiona McMurray[1], Christophe Girard[2], Gareth T Banks[1], Lydia Teboul[1], Sara Wells[1], Jens C Brüning[3], Patrick M Nolan[1], Frances M Ashcroft[2] & Roger D Cox[1]

Genome-wide association studies have identified SNPs within *FTO*, the human fat mass and obesity–associated gene, that are strongly associated with obesity. Individuals homozygous for the at-risk rs9939609 A allele weigh, on average, ~3 kg more than individuals with the low-risk T allele. Mice that lack FTO function and/or *Fto* expression display increased energy expenditure and a lean phenotype. We show here that ubiquitous overexpression of *Fto* leads to a dose-dependent increase in body and fat mass, irrespective of whether mice are fed a standard or a high-fat diet. Our results suggest that increased body mass results primarily from increased food intake. Mice with increased *Fto* expression on a high-fat diet develop glucose intolerance. This study provides the first direct evidence that increased *Fto* expression causes obesity in mice.

Up to 58% of the world's adult population is predicted to be overweight or obese by 2030 (ref. 1). Obesity predisposes to numerous diseases, including heart disease, type 2 diabetes and cancer; thus, understanding how body weight is regulated is of major scientific, health and economic importance. Genome-wide association studies have revealed that SNPs (including rs9939609, rs17817449, rs3751812, rs1421085 and rs9930506) in intron 1 of *FTO* are associated with an increased risk of obesity[2–5]. Approximately 16% of individuals of European descent are homozygous for the at-risk allele, weighing on average ~3 kg more than controls[4,5]. Evidence suggests that these individuals also exhibit increased food intake[6–13].

FTO is an AlkB-like 2-oxoglutarate–dependent nucleic acid demethylase[14–16] with a strong preference for 3-methylthymidine and 3-methyluracil in single-stranded DNA and RNA, respectively, owing to unique structural features[17]. A human *FTO* mutation (resulting in the p.Arg316Gln alteration) that inhibits catalytic activity results in an autosomal recessive lethal syndrome[15].

Mice lacking *Fto* show increased postnatal lethality, postnatal growth retardation, a reduced amount of adipose tissue and spontaneous locomotor activity, increased energy expenditure, and relative hyperphagia[18]. A dominant mutation (resulting in p.Ile367Phe) in the mouse *Fto* gene that reduces its DNA demethylation activity also results in reduced fat mass[19]. Taken together, these studies in the mouse suggest that loss of *Fto* expression and/or FTO function protects against obesity.

FTO is ubiquitously expressed in the embryo and adult[4]. High *Fto* mRNA levels are observed in the brain, including the cerebellum, hippocampus and hypothalamus[14,20,21]. In humans, *FTO* mRNA levels are higher in males and are positively correlated with body mass index (BMI) in adipose tissue[22] (although, see ref. 23 for an exception). *FTO* mRNA expression is also greater in subcutaneous adipose tissue (SAT)[24–26] of obese individuals compared to that of controls.

The association between brain *Fto* mRNA levels and food intake is controversial. Both increases (in rat[27] in the hypothalamus) and decreases (in mice[14,28] in the arcuate nucleus) in *Fto* mRNA levels have been reported to be linked to fasting. Direct manipulation of *Fto* RNA levels in the arcuate nucleus of rats by adenoviral infection of *Fto* or by small interfering RNA (siRNA) against *Fto* influences food intake; reduction in *Fto* expression leads to increased food intake and enhanced expression leads to decreased food intake[29]. Notably, mice with the p.Ile367Phe alteration did not show detectable altered food intake[19].

Taken together, these data demonstrate that the role of FTO in food intake in either humans or mice is ambiguous. Many[6,8,9,11], but not all[12,30,31], studies suggest that food intake is greater in humans who carry at-risk *FTO* SNPs. A confounder in obesity studies is that increased body mass requires increased energy expenditure for locomotion and potentially increased energy intake to match, making it difficult to determine the cause and effect of obesity phenotypes. The effects of loss of FTO function in rodents also remains unclear; deletion of the gene is reported to cause relative hyperphagia[18], whereas reduced demethylation activity had no effect on food intake[19]. This raises the question of whether increased *FTO* expression alters food intake and body weight in humans.

There is now the first evidence that primary transcripts containing an at-risk A allele at rs9939609 are more abundant than those with the T allele in blood and fibroblast RNA samples from several normal-weight (BMI 18.5–25.0 kg m^{-2}) individuals, suggesting that increased expression of *FTO* may be correlated with obesity[32]. To test

[1]MRC Harwell, Metabolism and Inflammation, Harwell Science and Innovation Campus, Harwell, UK. [2]Henry Wellcome Centre for Gene Function, Department of Physiology, Anatomy and Genetics, University of Oxford, Oxford, UK. [3]Center of Molecular Medicine Cologne (CMMC) and Cologne Excellence Cluster on Cellular Stress Responses in Aging-Associated Diseases (CECAD), University of Cologne, Cologne, Germany. Correspondence should be addressed to R.D.C. (r.cox@har.mrc.ac.uk).

Received 16 February; accepted 19 October; published online 14 November 2010; doi:10.1038/ng.713

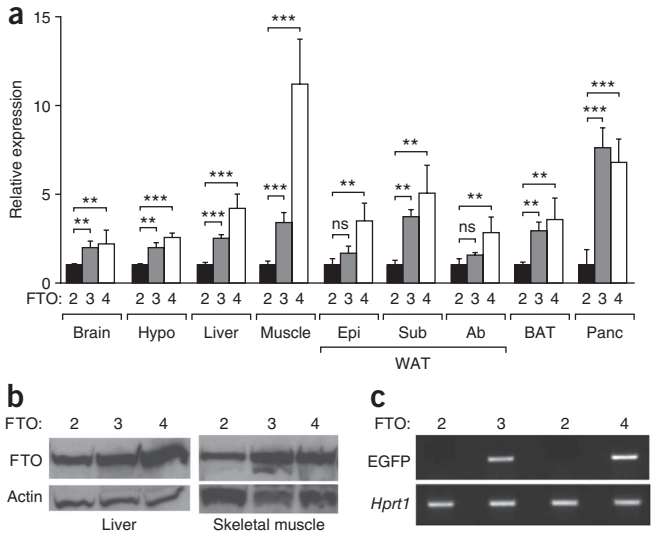

Figure 1 Generation of a mouse model overexpressing *Fto*. (**a**) Relative *Fto* expression in the indicated tissues of FTO-2 ($n = 10$), FTO-3 ($n = 10$) and FTO-4 ($n = 10$) mice. Ab, abdominal; BAT, brown adipose tissue; Epi, epigonadal; Hypo, hypothalamus; Panc, pancreas, Sub, subcutaneous; WAT, white adipose tissue. Data are expressed as mean ± s.e.m. $^{**}P < 0.01$; $^{***}P < 0.0001$; ns, nonsignificant. (**b**) Representative protein blots of FTO and actin (loading control) from skeletal muscle and liver from FTO-2, FTO-3 and FTO-4 mice. (**c**) RT-PCR of Egfp using brain cDNA prepared from FTO-2, FTO-3 and FTO-4 mice. *Hprt1*, encoding hypoxanthine-guanine phosphoribosyltransferase, is included as a control.

this hypothesis, we compared the effects of different copy numbers of the *Fto* gene using mouse models. Our data provide evidence that enhanced expression of *Fto* causes obesity.

RESULTS

To test the hypothesis that upregulation of *FTO* expression causes obesity, we generated mice that globally expressed either one or two additional copies of the *Fto* gene (**Supplementary Fig. 1** and Online Methods). We refer to these as FTO-3 and FTO-4 mice (as they have either three or four copies of *Fto* in total), and we refer to wild-type mice as FTO-2 mice.

Fto overexpression

Using quantitative RT–PCR (qRT-PCR) we showed increased *Fto* mRNA expression in multiple tissues of mice carrying additional copies of the *Fto* gene (**Fig. 1a**). In FTO-3 mice this increase was largest in the pancreas (~8-fold), whereas in FTO-4 mice, we found the greatest increase in expression (~11-fold) to be in skeletal muscle, followed by the pancreas. We used protein blot analysis to confirm that FTO protein was overexpressed in skeletal muscle and liver (**Fig. 1b**); this increase ranged from 1.9-fold in skeletal muscle of FTO-3 mice to 2.3-fold in FTO-4 mouse liver. We also confirmed expression of the EGFP reporter by RT-PCR (**Fig. 1c**).

Dose-dependent *Fto* expression affects body weight

Mice carrying additional copies of the *Fto* gene exhibited increased body weight (**Fig. 2**). On a standard diet, female FTO-3 mice diverged from the wild type at ~5 weeks, becoming 11% ± 3% (s.e.m.) heavier than FTO-2 littermates by 20 weeks of age (**Fig. 2a** and **Fig. 3a**). Female FTO-4 mice showed earlier divergence from the wild type (4 weeks of age; **Fig. 2a**) and were 22% ± 4% heavier at 20 weeks (**Fig. 3a**). We obtained similar results for male FTO-3 and FTO-4 mice, although the increase in weight was slightly less than for female mice; by 20 weeks of age, male FTO-3 and FTO-4 mice were 7% ± 2% and 10% ± 1% heavier, respectively, than their FTO-2 littermates (**Fig. 2c** and **Fig. 3a**).

In all genotypes, a high-fat diet (HFD) led to increased body weight. However, the effect was greater in mice overexpressing *Fto* (**Fig. 2b**,**d**). After 20 weeks, female FTO-3 and FTO-4 mice were 9% ± 2% and 18% ± 6% heavier, respectively, than FTO-2 mice (**Fig. 2b** and **Fig. 3a**). Male mice also showed an increased body weight (7% ± 2% for FTO-3 and 13% ± 3% for FTO-4 mice) (**Fig. 2d** and **Fig. 3a**). Body length was not different from the wild type in FTO-3 and FTO-4 mice (data not shown).

Dose-dependent expression of *Fto* affects fat mass

Mice overexpressing *Fto* showed increased fat mass (**Fig. 3b** and **Supplementary Fig. 2**). Twenty-week-old female FTO-3 mice on a standard diet displayed a 42% ± 8% increase in fat mass, and FTO-4 mice displayed a 85% ± 9.5% increase in fat mass compared to FTO-2 control mice (**Fig. 3b**). Male FTO-3 and FTO-4 mice showed similar increases in fat mass (**Fig. 3b**). A greater increase in fat mass was seen on a high-fat diet, with similar increases in FTO-3 and FTO-4 mice relative to wild-type mice. This was again particularly pronounced in

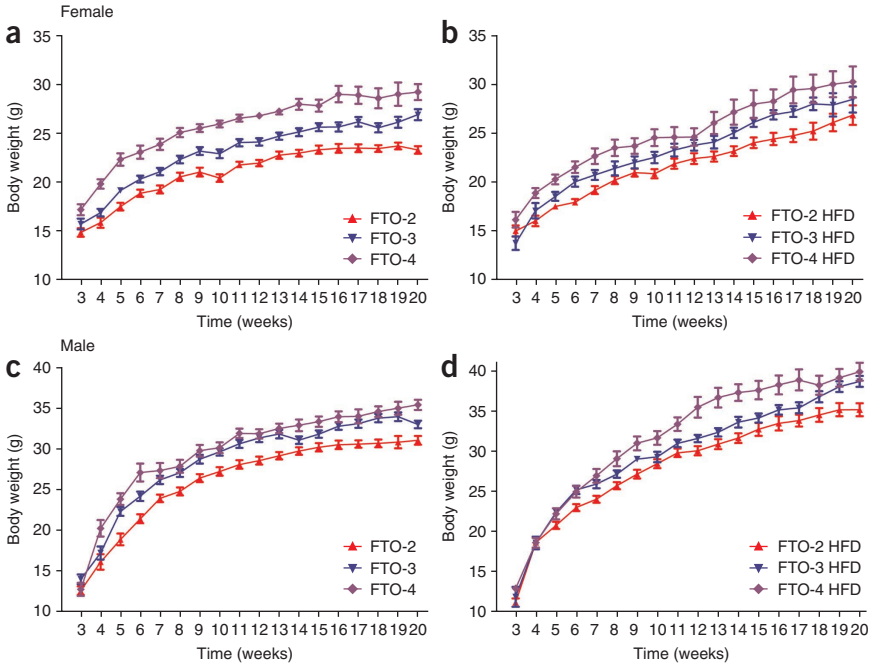

Figure 2 *Fto* dose-dependent increases in body weight are observed in male and female mice on standard (SD) and high-fat (HFD) diets. (**a**) Females on SD. FTO-2 (wild type, $n = 16$), FTO-3 ($n = 28$, $P = 0.0003$) and FTO-4 ($n = 16$, $P < 0.0001$). (**b**) Females on HFD. FTO-2 ($n = 15$), FTO-3 ($n = 14$, $P = 0.04$) and FTO-4 ($n = 15$, $P = 0.002$). (**c**) Males on SD. FTO-2 ($n = 16$), FTO-3 ($n = 31$, $P = 0.001$) and FTO-4 ($n = 16$, $P = 0.0001$). (**d**) Males on HFD. FTO-2 ($n = 18$), FTO-3 ($n = 15$, $P = 0.01$) and FTO-4 ($n = 16$, $P < 0.0001$). Data are expressed as mean ± s.e.m. Statistical analysis was performed using a repeated measures analysis of variance. All P values are against FTO-2.

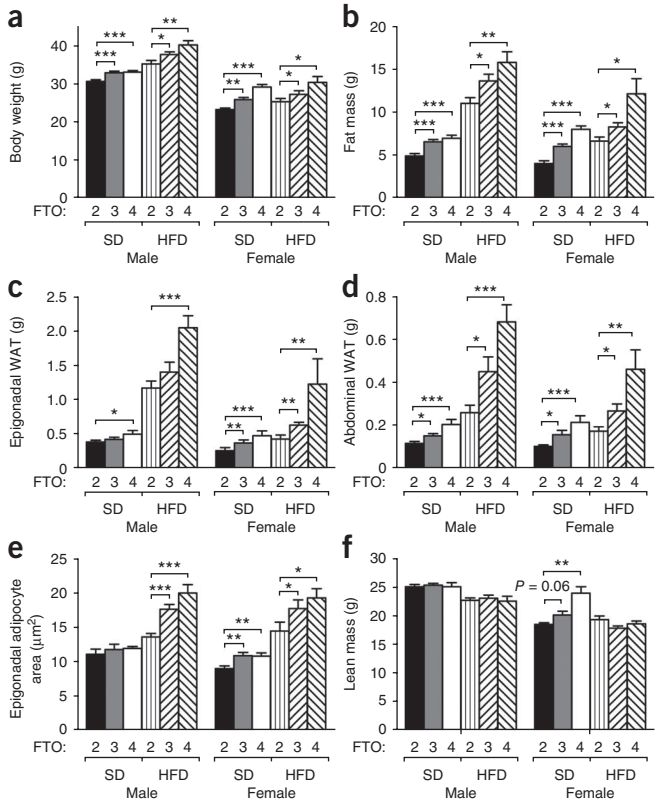

Figure 3 Body composition varies with *Fto* copy number. (**a**) Body weight of 20-week-old male and female mice on a standard (SD) and high-fat diet (HFD). Males on SD: FTO-2 ($n = 16$), FTO-3 ($n = 31$) and FTO-4 ($n = 15$). Males on HFD: FTO-2 ($n = 18$), FTO-3 ($n = 15$) and FTO-4 ($n = 16$). Females on SD: FTO-2 ($n = 16$), FTO-3 ($n = 28$) and FTO-4 ($n = 16$). Females on HFD: FTO-2 ($n = 15$), FTO-3 ($n = 14$) and FTO-4 ($n = 15$). (**b**) Total fat mass measured by dual-energy X-ray absorptiometry (DEXA) scanning in male and female mice on SD and HFD. Males on SD: FTO-2 ($n = 16$), FTO-3 ($n = 30$) and FTO-4 ($n = 15$). Males on HFD: FTO-2 ($n = 17$), FTO-3 ($n = 15$) and FTO-4 ($n = 16$). Females on SD: FTO-2 ($n = 16$), FTO-3 ($n = 28$) and FTO-4 ($n = 16$). Females on HFD: FTO-2 ($n = 16$), FTO-3 ($n = 14$) and FTO-4 ($n = 15$). (**c**,**d**) Weights of epigonadal WAT (**c**) and abdominal WAT (**d**) in mice overexpressing *Fto*. Males on SD: FTO-2 ($n = 16$), FTO-3 ($n = 21$) and FTO-4 ($n = 15$). Males on HFD: FTO-2 ($n = 15$), FTO-3 ($n = 14$) and FTO-4 ($n = 14$). Females on SD: FTO-2 ($n = 15$), FTO-3 ($n = 28$) and FTO-4 ($n = 15$). Females on HFD: FTO-2 ($n = 12$), FTO-3 ($n = 14$) and FTO-4 ($n = 14$). (**e**) Epigonadal adipocyte area is increased in female mice on both SD and HFD and in males on a HFD ($n = 5$ in each case). (**f**) Lean body mass in male and female mice on SD and HFD. Same mouse numbers as in **b**. Data in **a**–**f** are expressed as mean ± s.e.m. $^*P < 0.05$; $^{**}P < 0.01$; $^{***}P < 0.0001$.

female mice, where fat mass was 18% ± 7% (FTO-3) and 68% ± 21% (FTO-4) greater than that of the wild type at 20 weeks (**Fig. 3b**). In male mice, fat mass was also increased, being 24% ± 7% (FTO-3) and 43% ± 10% (FTO-4) greater than wild type (**Fig. 3b**).

We observed similar correlations between *Fto* copy number and the weight of dissected fat pads. Thus, epigonadal and abdominal white adipose tissues (WATs) were heavier in female FTO-3 and FTO-4 mice than in FTO-2 mice (**Fig. 3c**,**d**). We found similar results in male mice, except that epigonadal WAT was not increased in FTO-3 mice. High-fat feeding further exacerbated the dose-dependent effect of *Fto* overexpression on epigonadal and abdominal WAT in both male and female mice (**Fig. 3c**,**d**). Hematoxylin and eosin histological analysis of epigonadal WAT (**Supplementary Fig. 3a**) showed an increase in adipocyte size at 20 weeks of age on both standard and high-fat diets in females and on a high-fat diet in males when assessed quantitatively through the adipocyte area (**Fig. 3e**).

Lean mass was affected to a lesser extent when *Fto* was overexpressed, but female FTO-4 mice showed a 21% ± 9% increase in lean mass on a standard diet (**Fig. 3f**). We found no significant difference in lean mass between FTO-2 and FTO-3 or FTO-4 mice on a high-fat diet (**Fig. 3f** and **Supplementary Fig. 2b**,**d**).

Regression analysis showed that mice overexpressing *Fto* have a different body composition compared to wild-type mice, showing a higher fat-to-lean tissue mass ratio (**Supplementary Fig. 2**).

Fto overexpression increases food intake

Many human studies have suggested that individuals carrying the at-risk *FTO* allele exhibit increased energy intake[6–11,13]. FTO-3 and FTO-4 mice on both standard and high-fat diets consumed more than FTO-2 mice at 10 weeks and at 19 weeks of age (**Supplementary Fig. 3b**). The relative increase in food intake displayed by FTO-3 and FTO-4 mice compared to their wild-type littermates was even greater on a high-fat diet (**Supplementary Fig. 3b**). This was maintained when

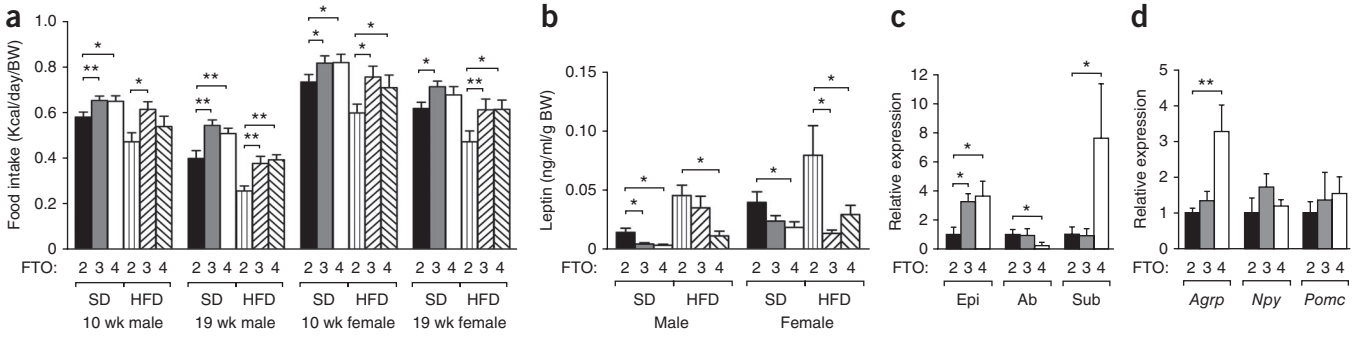

Figure 4 Effects of *Fto* on energy intake and plasma leptin. (**a**) Food intake over 24 h normalized to body weight (BW), measured in 10-week-old and 19-week-old mice. Males on SD: FTO-2 ($n = 16$), FTO-3 ($n = 31$) and FTO-4 ($n = 16$). Males on HFD: FTO-2 ($n = 18$), FTO-3 ($n = 15$) and FTO-4 ($n = 16$). Females on SD: FTO-2 ($n = 16$), FTO-3 ($n = 28$) and FTO-4 ($n = 16$). Females on HFD: FTO-2 ($n = 15$), FTO-3 ($n = 14$) and FTO-4 ($n = 15$). (**b**) Plasma leptin levels at 8 weeks of age adjusted for BW following an overnight 16-h fast. Males on SD: FTO-2 ($n = 14$), FTO-3 ($n = 25$) and FTO-4 ($n = 14$). Males on HFD: FTO-2 ($n = 12$), FTO-3 ($n = 12$) and FTO-4 ($n = 12$). Females on SD: FTO-2 ($n = 16$), FTO-3 ($n = 25$) and FTO-4 ($n = 14$). Females on HFD: FTO-2 ($n = 13$), FTO-3 ($n = 10$) and FTO-4 ($n = 10$). (**c**) Relative *Lep* (Leptin) gene expression in 20-week-old female epigonadal (Epi), abdominal (Ab) and subcutaneous (sub) WAT. FTO-2 ($n = 10$), FTO-3 ($n = 10$) and FTO-4 ($n = 10$). (**d**) Relative gene expression of hypothalamic neuropeptides. FTO-2 ($n = 10$), FTO-3 ($n = 10$) and FTO-4 ($n = 10$) mice. Data in **a**–**d** are expressed as mean ± s.e.m. $^*P < 0.05$; $^{**}P < 0.01$.

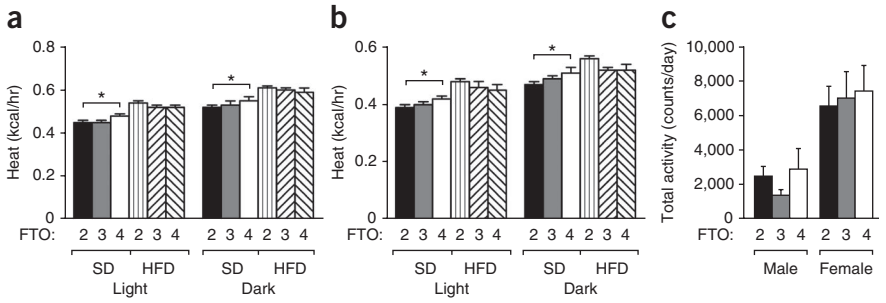

Figure 5 Effects of *Fto* on energy expenditure and physical activity. (**a**–**c**) Heat production over a 22-h period during the light and dark phases for 18-week-old male (**a**) and female (**b**) mice on a standard (SD) or high-fat diet (HFD). Males on SD: FTO-2 ($n = 15$), FTO-3 ($n = 25$) and FTO-4 ($n = 16$). Males on HFD: FTO-2 ($n = 12$), FTO-3 ($n = 12$) and FTO-4 ($n = 15$). Females on SD: FTO-2 ($n = 16$), FTO-3 ($n = 22$) and FTO-4 ($n = 15$). Females on HFD: FTO-2 ($n = 12$), FTO-3 ($n = 13$) and FTO-4 ($n = 14$). (**c**) Physical activity was measured as the number of rotations of an activity wheel in a 7-d period, following a 3-d entrainment period. Males and females combined: FTO-2 ($n = 7$), FTO-3 ($n = 7$) and FTO-4 ($n = 6$). Data in **a**–**c** are expressed as mean ± s.e.m. *$P < 0.05$.

food intake was normalized to body weight for FTO-3 and FTO-4 mice, with the exception of FTO-4 female mice on a standard diet, in which this increase in food intake was reduced to a trend (**Fig. 4a**).

We confirmed these differences by regression analysis against body weight at 10 weeks, which showed increased food intake at all body weights for FTO-3 and FTO-4 mice (**Supplementary Fig. 4**). At 20 weeks, a similar pattern was evident for males (**Supplementary Fig. 5a**,**b**). Further, in 20-week-old FTO-4 males, food intake was elevated regardless of lean mass, fat mass (a trend on a standard diet, significant ($P < 0.05$) on a high-fat diet) or body composition (defined as the fat mass/lean mass (FM/LM) ratio; **Supplementary Fig. 5**). These trends were less clear in females (**Supplementary Fig. 6** and **Supplementary Note**).

As food intake is under endocrine and neuronal control and is influenced by leptin, we measured plasma leptin levels. At 8 weeks of age, circulating leptin levels after a 16-h overnight fast, either as raw data (data not shown) or corrected for body weight, were significantly lower in male and female FTO-4 mice than in FTO-2 mice, whether mice were maintained on a standard or high-fat diet (**Fig. 4b**). This was largely confirmed by regression analysis against body weight (**Supplementary Fig. 7a**,**b** and **Supplementary Fig. 8a**,**b**).

There was no significant difference in circulating leptin at 20 weeks of age either as raw data (data not shown) or corrected for fat mass, with the exception of FTO-3 males on a standard diet, which showed a significant increase in relative leptin levels (with a trend for an increase ($P = 0.07$) observed for FTO-4 males (**Supplementary Fig. 3c**, **Supplementary Fig. 7c** and **Supplementary Fig. 8c**)). Regression analysis showed a clear positive correlation between leptin levels and fat mass in mice on a high-fat diet, explaining 76% ($P = 0.0009$) and 44% ($P = 0.0018$) of the variation in leptin for FTO-4 females and males, respectively (**Supplementary Fig. 7d** and **Supplementary Fig. 8d**). Consistent with the elevated circulating leptin, leptin mRNA expression was higher in epigonadal and subcutaneous WAT but was reduced in abdominal WAT of 20-week-old FTO-4 mice (**Fig. 4c**).

Hypothalamic expression of *Agrp*, which encodes agouti-related protein, was elevated in fasting in 20-week-old FTO-4 male mice, but *Npy* (encoding neuropeptide Y) and *Pomc* (encoding proopiomelanocortin) levels were unaffected (**Fig. 4d**).

Fto and alterations in energy expenditure

Previous studies with *Fto* knockout[18] and *Fto* p.Ile367Phe mutant mice[19] suggested that an increased metabolic rate might underlie their lean phenotype. We therefore used indirect calorimetry to assess metabolic rate in 18-week-old mice.

FTO-4 mice showed a significant increase in energy expenditure (heat, kcal h^{-1}) on a standard diet during both light and dark periods, but we observed no other differences (**Fig. 5a**,**b**). We then carried out multiple regression analysis for energy expenditure to assess the effect of potential explanatory variables (weight, lean mass, fat mass, sex, genotype and diet) using an additive linear model (**Supplementary Table 1**). We identified lean body mass ($P = 0.0446$) and high-fat diet ($P = 4.2 \times 10^{-7}$) as predictors. We then used a model that automatically selected relevant variables, identifying weight ($P = 0.0077$), lean mass ($P = 0.0003$) and high-fat diet ($P = 6.05 \times 10^{-8}$) as the main predictor of energy expenditure (adjusted r^2 correlation coefficient 0.441, $P \leq 2.2 \times 10^{-16}$). We confirmed these results using a robust fit linear model (data not shown). When tested alone, genotype was not a predictor of energy expenditure (data not shown).

There was no significant change in respiratory exchange ratio (RER) for FTO-3 or FTO-4 mice on either a standard or high-fat diet (data not shown).

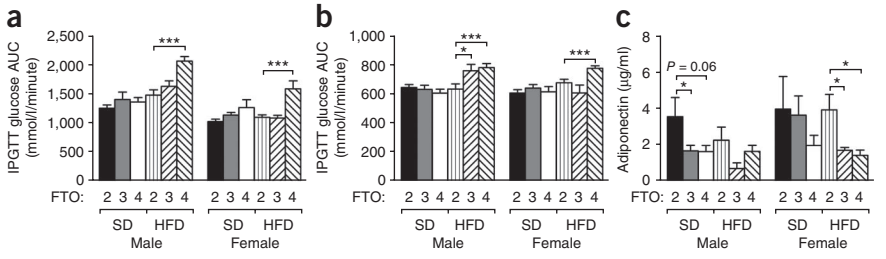

Figure 6 Glucose homeostasis and *Fto* overexpression. (**a**) Area under the curve (AUC) during a 120-min IPGTT in 12-week-old mice. Males on SD: FTO-2 ($n = 15$), FTO-3 ($n = 25$) and FTO-4 ($n = 16$). Males on HFD: FTO-2 ($n = 12$), FTO-3 ($n = 13$) and FTO-4 ($n = 12$). Females on SD: FTO-2 ($n = 16$), FTO-3 ($n = 22$) and FTO-4 ($n = 15$). Females on HFD: FTO-2 ($n = 12$), FTO-3 ($n = 12$) and FTO-4 ($n = 13$). (**b**) AUC analysis for glucose during a 30-min IPGTT in 16-week-old mice. Males on SD: FTO-2 ($n = 15$), FTO-3 ($n = 23$) and FTO-4 ($n = 15$). Males on HFD: FTO-2 ($n = 12$), FTO-3 ($n = 12$) and FTO-4 ($n = 14$). Females on SD: FTO-2 ($n = 16$), FTO-3 ($n = 22$) and FTO-4 ($n = 15$). Females on HFD: FTO-2 ($n = 12$), FTO-3 ($n = 11$) and FTO-4 ($n = 15$). (**c**) Adiponectin levels at 20 weeks of age following a 6-h light-phase fast. Males on SD: FTO-2 ($n = 12$), FTO-3 ($n = 22$) and FTO-4 ($n = 10$). Males on HFD: FTO-2 ($n = 12$), FTO-3 ($n = 10$) and FTO-4 ($n = 10$). Females on SD: FTO-2 ($n = 11$), FTO-3 ($n = 22$) and FTO-4 ($n = 9$). Females on HFD: FTO-2 ($n = 10$), FTO-3 ($n = 9$) and FTO-4 ($n = 10$). Data in **a**–**c** are expressed as mean ± s.e.m. *$P < 0.05$; ***$P < 0.0001$.

Table 1 Plasma biochemistry in 20-week-old female mice

		FTO-2	FTO-3	FTO-4	*t* test	
	Units	$n = 16$	$n = 28$	$n = 17$	FTO-2 vs. FTO-3 (P)[a]	FTO-2 vs. FTO-4 (P)[a]
ALP	U l^{-1}	84.7 ± 6	86 ± 4	87 ± 8	0.8696	0.8173
ALT	U l^{-1}	42 ± 5	42 ± 4	70 ± 17	0.8913	**0.0473**
AST	U l^{-1}	134 ± 20	166 ± 15	192 ± 41	0.2198	0.1680
Albumin	g l^{-1}	30 ± 1.6	27 ± 0.4	26 ± 0.6	**0.0229**	0.0785
Cholesterol[b]	mmol l^{-1}	2.4 ± 0.19	2.6 ± 0.13	2.1 ± 0.14	0.3435	0.6101
HDL-C[b]	mmol l^{-1}	1.2 ± 0.1	1.6 ± 0.1	1.5 ± 0.1	**0.0320**	**0.0460**
LDL-C[b]	mmol l^{-1}	0.68 ± 0.17	0.39 ± 0.02	0.33 ± 0.22	**0.0347**	**0.0657**
Glucose	mmol l^{-1}	16.8 ± 0.7	19.6 ± 0.8	15.9 ± 1.7	**0.0137**	0.5247
Triglycerides	mmol l^{-1}	0.69 ± 0.04	0.94 ± 0.06	0.80 ± 0.03	**0.0074**	**0.0472**
Glycerol	µmol l^{-1}	562 ± 25	577 ± 24	543 ± 19	0.7683	0.5745
FFA	mmol l^{-1}	0.82 ± 0.06	1.07 ± 0.06	1.11 ± 0.08	**0.0273**	**0.0320**
LDH	U l^{-1}	680 ± 72	743 ± 54	879 ± 122	0.5240	0.2366
Amylase	U l^{-1}	580 ± 22	632 ± 78	743 ± 109	0.1420	0.1819
CK	U l^{-1}	207 ± 38	367 ± 43	450 ± 73	**0.0308**	**0.0147**

Plasma biochemistry in 20-week-old female FTO-2, FTO-3 and FTO-4 mice on a standard diet. All data are given as mean ± s.e.m. ALP, alkaline phosphatase; ALT, alanine aminotransferase; AST, aspartate aminotransferase; FFA, free fatty acids; LDH, lactate dehydrogenase; CK, creatine kinase.
[a]Bold text, $P < 0.05$. [b]Cholesterol, total cholesterol; HDL-C, HDL-cholesterol; LDL, LDL-cholesterol.

Fto has no effect on activity or circadian period

To assess whether reduced locomotor activity contributes to the obese phenotype of mice overexpressing *Fto*, we measured activity at 12 weeks of age by wheel running. We found no significant difference in wheel running during a 7-d period in either female or male FTO-3 or FTO-4 mice compared to FTO-2 mice (**Fig. 5c**). There was also no difference in the length of wheel-running time during circadian challenges, including a shift to constant darkness or constant light, in mice overexpressing FTO compared to their wild-type littermates (**Supplementary Fig. 9a–d**).

An open-field anxiety paradigm was used to test a combination of locomotor activity, exploratory drive and other aspects of anxiety at 10 weeks of age. Female FTO-3 and FTO-4 mice showed no difference in total activity, as determined by the distance moved during the period (**Supplementary Fig. 9e**), but female FTO-4 mice spent less time in the center of the open field, suggesting that they may be more anxious (**Supplementary Fig. 9 f–h**). We observed no significant phenotype in male FTO-3 and FTO-4 mice (data not shown). Following 4 weeks of access to running wheels and the same light and dark regime, FTO-3 and FTO-4 mice showed increased body mass and fat mass at 12 weeks of age consistent with the phenotype observed at 20 weeks of age (**Supplementary Table 2**).

Dose-dependent effect of *Fto* expression on glucose tolerance

We assessed glucose homeostasis at 12 weeks of age with a 120-min intraperitoneal glucose tolerance test (IPGTT) and examined the mice again at 16 weeks of age with a 30-min IPGTT (data not shown). We quantified glucose tolerance by measuring the area under the curve (AUC) relating plasma glucose levels to time. We observed no significant difference in AUC at 12 weeks between mice expressing different numbers of the *Fto* gene fed a standard diet (**Fig. 6a**). Notably, when challenged with a high-fat diet, FTO-4 mice exhibited a reduction in glucose tolerance compared to wild-type mice, as shown by an increase in glucose AUC at 12 weeks (**Fig. 6a**) and at 16 weeks (**Fig. 6b**).

Plasma insulin levels were unchanged at 8 weeks (fasting), 16 weeks (over a 30-min IPGTT) and 20 weeks (fasting) of age in male and female FTO-3 and FTO-4 mice on a standard diet (data not shown). However, male FTO-4 mice on a high-fat diet had elevated fasting insulin at 16 weeks of age (1.05 µg l^{-1} ± 0.22 µg l^{-1} compared to 0.64 µg l^{-1} ± 0.09 µg l^{-1} for wild type, $P = 0.025$). Female FTO-3 and FTO-4 mice had lower adiponectin levels than wild-type mice on a high-fat diet but not on a standard diet (**Fig. 6c**), whereas the reverse was found for male mice (**Fig. 6c**).

Fto overexpression alters plasma biochemistry

Plasma biochemistry measured in 20-week-old female mice is shown in **Table 1**. Circulating plasma levels of triglycerides, free fatty acids (FFA) and high-density lipoprotein (HDL) cholesterol were significantly greater in FTO-3 and FTO-4 mice than in FTO-2 mice, but LDL cholesterol was reduced. We assessed liver function by measuring alkaline phosphatase (ALP), alanine aminotransferase (ALT) and aspartate aminotransferase (AST) levels. FTO-4 mice exhibited significantly increased ALT and lower albumin levels (**Table 1**). Creatine kinase was increased in FTO-3 and FTO-4 mice on standard and high-fat diets. We found no significant differences in males (data not shown).

DISCUSSION

Our data show that FTO is directly involved in the regulation of energy intake and metabolism in mice, and that enhanced expression of *Fto* leads to increased food intake and obesity.

Overexpression of *Fto* caused a dose-dependent increase in body weight and fat mass. The increase in weight of mice overexpressing *Fto* seems to be largely due to an increase in fat mass, as it is for humans carrying the at-risk allele[4,33]. On a high-fat diet, female FTO-4 mice were 18% heavier, and FTO-3 mice were 9%, heavier than controls; on a standard diet, these mice were 22% heavier and 11% heavier, respectively. In comparison, humans carrying two at-risk alleles (for example, the rs9939609 A allele) are on average ~3.4% heavier (assuming an average adult body weight of 90 kg) than those carrying the low-risk alleles. Thus, FTO activity and expression in our mice is likely to be greater than in at-risk humans, enabling the phenotype to be dissected more easily.

Previous work showed that increased body mass in rs9939609 A allele carriers manifests during childhood[4]. Likewise, in FTO-4 mice, the increase in body weight was present early, being significantly different from that of the wild type at 4 weeks of age on a standard diet.

Overexpression of *Fto* led to a marked increase in food intake. This was observed on both standard and high-fat diets and at both

10 weeks and 19 weeks of age. We conclude that the increase in food intake contributes to the increased fat mass and body weight of FTO-3 and FTO-4 mice. Regression analysis at 20 weeks showed that food intake in male FTO-4 mice was elevated regardless of body weight, lean mass, fat mass or body composition (FM/LM). Mice overexpressing *Fto* reduced their food intake on a high-fat diet, relative to the standard diet, indicating that their energy intake was still regulated but that increased *Fto* expression had shifted the set point to a higher level. Most studies in humans report that at-risk SNPs enhance energy intake[6–9,11], with some other studies finding no evidence of any effect on food intake[12,30,31]. Manipulation of *Fto* levels in the arcuate nucleus using adenoviral technology decreased food intake, in contrast to our observations[29]. However, in the *Fto* overexpression mice used in this study, other tissues may also influence food intake, such as additional brain regions, the gut and adipose tissue.

Leptin, a hormone released from adipocytes that acts in the brain, is a potent regulator of food intake. We observed a reduction in circulating leptin levels at 8 weeks of age in mice overexpressing *Fto*, with the greatest reduction seen in FTO-4 mice. It is therefore possible that the hyperphagia of FTO-3 and FTO-4 mice is due to an FTO-dependent reduction in leptin concentration. However, we did not observe these differences in 20-week-old mice, and leptin levels correlated well with the increased fat mass. In human population studies, individuals with the *FTO* at-risk allele showed increased plasma leptin[31,34], but this effect disappeared when adjusted for BMI[34], suggesting that this is a result of increased adiposity.

Multivariate regression analysis in the mice used in this study indicates that the most significant predictor of energy expenditure is a high-fat diet. The high-fat diet may increase body weight, which subsequently requires greater energy expenditure for physical activity (**Fig. 5a**,**b**). Other significant determinants of energy expenditure were lean mass and weight. Notably, we did not detect genotype or sex effects in this global analysis of energy expenditure determinants. We conclude that, in these mouse models, energy expenditure is not a major determinant of the obese phenotype. Although humans carrying the *FTO* at-risk allele exhibited increased resting energy expenditure[31,35,36], this difference was abolished when adjusted for fat mass (or lean body mass)[31,35,36].

We found no effect of *Fto* copy number on spontaneous locomotor activity in mice. Similarly, in humans, there is no association between *FTO* risk alleles and the extent of leisure time physical activity[35,37] (although physical activity may modify the effect of the *FTO* risk allele, as BMI was attenuated in high physical activity groups[38]).

Obesity strongly increases the risk of type 2 diabetes. Consistent with this, FTO-4 mice showed marked glucose intolerance on a high-fat diet.

The ubiquitous unregulated overexpression in our mice does not necessarily recapitulate normal expression patterns, although *FTO* is expressed ubiquitously[4,14]. The functional consequences of the human risk alleles are likely to be more restricted than our promiscuous allele. Our analysis was carried out after the body weight had already diverged and could potentially be confounded by these changes.

We show that increased expression of *Fto* leads to increased fat mass and obesity through hyperphagia. These data suggest that the at-risk SNPs in the human *FTO* gene may enhance the expression and/or activity of FTO. Our data further suggest that anti-obesity drugs targeted to FTO should be designed to reduce FTO expression or activity and predict that their effects *in vivo* will largely act by reducing appetite.

URLs. Standardized protocols for EMPReSS, http://empress.har.mrc.ac.uk/; R, http://www.r-project.org/.

METHODS

Methods and any associated references are available in the online version of the paper at http://www.nature.com/naturegenetics/.

Note: Supplementary information is available on the Nature Genetics website.

ACKNOWLEDGMENTS

We thank the UK Medical Research Council (MRC) (to L.M., L.T., S.W., P.M.N., G.T.B., R.D.C. and studentships to C.C. and F.M.) and the UK Royal Society (research professorship to F.M.A.) for personnel support, and the MRC and Wellcome Trust for financing the research (R.D.C. and F.M.A.). We thank C. Holmes, G. Nicholson and O. Espinosa for help with multiple regression analysis using R.

AUTHOR CONTRIBUTIONS

C.C., R.D.C. and F.M.A. planned the project and wrote the manuscript. C.C., L.M. and F.M. carried out the whole-animal experiments. P.M.N., S.W. and G.T.B. carried out the behavioral and circadian studies. J.C.B. and C.G. provided overexpression vector design, construction and methods. L.T. and C.C. carried out the transgenic work.

COMPETING FINANCIAL INTERESTS

The authors declare no competing financial interests.

Published online at http://www.nature.com/naturegenetics/.
Reprints and permissions information is available online at http://npg.nature.com/reprintsandpermissions/.

1. Kelly, T., Yang, W., Chen, C.S., Reynolds, K. & He, J. Global burden of obesity in 2005 and projections to 2030. *Int. J. Obes.* **32**, 1431–1437 (2008).
2. Scuteri, A. *et al.* Genome-wide association scan shows genetic variants in the *FTO* gene are associated with obesity-related traits. *PLoS Genet.* **3**, e115 (2007).
3. Hinney, A. *et al.* Genome wide association (GWA) study for early onset extreme obesity supports the role of fat mass and obesity associated gene (*FTO*) variants. *PLoS ONE* **2**, e1361 (2007).
4. Frayling, T.M. *et al.* A common variant in the *FTO* gene is associated with body mass index and predisposes to childhood and adult obesity. *Science* **316**, 889–894 (2007).
5. Dina, C. *et al.* Variation in *FTO* contributes to childhood obesity and severe adult obesity. *Nat. Genet.* **39**, 724–726 (2007).
6. Cecil, J.E., Tavendale, R., Watt, P., Hetherington, M.M. & Palmer, C.N. An obesity-associated *FTO* gene variant and increased energy intake in children. *N. Engl. J. Med.* **359**, 2558–2566 (2008).
7. Haupt, A. *et al.* Variation in the *FTO* gene influences food intake but not energy expenditure. *Exp. Clin. Endocrinol. Diabetes* **117**, 194–197 (2009).
8. Speakman, J.R., Rance, K.A. & Johnstone, A.M. Polymorphisms of the *FTO* gene are associated with variation in energy intake, but not energy expenditure. *Obesity (Silver Spring)* **16**, 1961–1965 (2008).
9. Timpson, N.J. *et al.* The fat mass- and obesity-associated locus and dietary intake in children. *Am. J. Clin. Nutr.* **88**, 971–978 (2008).
10. Wardle, J. *et al.* Obesity associated genetic variation in *FTO* is associated with diminished satiety. *J. Clin. Endocrinol. Metab.* **93**, 3640–3643 (2008).
11. Wardle, J., Llewellyn, C., Sanderson, S. & Plomin, R. The *FTO* gene and measured food intake in children. *Int. J. Obes.* **33**, 42–45 (2009).
12. Tanofsky-Kraff, M. *et al.* The *FTO* gene rs9939609 obesity-risk allele and loss of control over eating. *Am. J. Clin. Nutr.* **90**, 1483–1488 (2009).
13. Sonestedt, E. *et al.* Fat and carbohydrate intake modify the association between genetic variation in the *FTO* genotype and obesity. *Am. J. Clin. Nutr.* **90**, 1418–1425 (2009).
14. Gerken, T. *et al.* The obesity-associated *FTO* gene encodes a 2-oxoglutarate-dependent nucleic acid demethylase. *Science* **318**, 1469–1472 (2007).
15. Boissel, S. *et al.* Loss-of-function mutation in the dioxygenase-encoding *FTO* gene causes severe growth retardation and multiple malformations. *Am. J. Hum. Genet.* **85**, 106–111 (2009).
16. Jia, G. *et al.* Oxidative demethylation of 3-methylthymine and 3-methyluracil in single-stranded DNA and RNA by mouse and human FTO. *FEBS Lett.* **582**, 3313–3319 (2008).
17. Han, Z. *et al.* Crystal structure of the FTO protein reveals basis for its substrate specificity. *Nature* **464**, 1205–1209 (2010).
18. Fischer, J. *et al.* Inactivation of the *Fto* gene protects from obesity. *Nature* **458**, 894–898 (2009).

19. Church, C. *et al.* A mouse model for the metabolic effects of the human fat mass and obesity associated *FTO* gene. *PLoS Genet.* **5**, e1000599 (2009).
20. Lein, E.S. *et al.* Genome-wide atlas of gene expression in the adult mouse brain. *Nature* **445**, 168–176 (2007).
21. Olszewski, P.K. *et al.* Hypothalamic FTO is associated with the regulation of energy intake not feeding reward. *BMC Neurosci.* **10**, 129 (2009).
22. Grunnet, L.G. *et al.* Regulation and function of FTO mRNA expression in human skeletal muscle and subcutaneous adipose tissue. *Diabetes* **58**, 2402–2408 (2009).
23. Klöting, N. *et al.* Inverse relationship between obesity and *FTO* gene expression in visceral adipose tissue in humans. *Diabetologia* **51**, 641–647 (2008).
24. Villalobos-Comparán, M. *et al.* The *FTO* gene is associated with adulthood obesity in the Mexican population. *Obesity (Silver Spring)* **16**, 2296–2301 (2008).
25. Wåhlén, K., Sjolin, E. & Hoffstedt, J. The common rs9939609 gene variant of the fat mass- and obesity-associated gene *FTO* is related to fat cell lipolysis. *J. Lipid Res.* **49**, 607–611 (2008).
26. Zabena, C. *et al.* The *FTO* obesity gene. Genotyping and gene expression analysis in morbidly obese patients. *Obes. Surg.* **19**, 87–95 (2009).
27. Fredriksson, R. *et al.* The obesity gene, *FTO*, is of ancient origin, up-regulated during food deprivation and expressed in neurons of feeding-related nuclei of the brain. *Endocrinology* **149**, 2062–2071 (2008).
28. Stratigopoulos, G. *et al.* Regulation of *Fto*/*Ftm* gene expression in mice and humans. *Am. J. Physiol. Regul. Integr. Comp. Physiol.* **294**, R1185–R1196 (2008).
29. Tung, Y.C. *et al.* Hypothalamic-specific manipulation of *Fto*, the ortholog of the human obesity gene *FTO*, affects food intake in rats. *PLoS ONE* **5**, e8771 (2010).
30. Hakanen, M. *et al. FTO* genotype is associated with body mass index after the age of seven years but not with energy intake or leisure-time physical activity. *J. Clin. Endocrinol. Metab.* **94**, 1281–1287 (2009).
31. Do, R. *et al.* Genetic variants of *FTO* influence adiposity, insulin sensitivity, leptin levels, and resting metabolic rate in the Quebec Family Study. *Diabetes* **57**, 1147–1150 (2008).
32. Berulava, T. & Horsthemke, B. The obesity-associated SNPs in intron 1 of the *FTO* gene affect primary transcript levels. *Eur. J. Hum. Genet.* **18**, 1054–1056 (2010).
33. Haupt, A. *et al.* Impact of variation in the *FTO* gene on whole body fat distribution, ectopic fat, and weight loss. *Obesity (Silver Spring)* **16**, 1969–1972 (2008).
34. Qi, L. *et al.* Fat mass-and obesity-associated (*FTO*) gene variant is associated with obesity: longitudinal analyses in two cohort studies and functional test. *Diabetes* **57**, 3145–3151 (2008).
35. Berentzen, T. *et al.* Lack of association of fatness-related *FTO* gene variants with energy expenditure or physical activity. *J. Clin. Endocrinol. Metab.* **93**, 2904–2908 (2008).
36. Goossens, G.H. *et al.* Several obesity- and nutrient-related gene polymorphisms but not *FTO* and *UCP* variants modulate postabsorptive resting energy expenditure and fat-induced thermogenesis in obese individuals: the NUGENOB study. *Int. J. Obes.* **33**, 669–679 (2009).
37. Jonsson, A. *et al.* Assessing the effect of interaction between an *FTO* variant (rs9939609) and physical activity on obesity in 15,925 Swedish and 2,511 Finnish adults. *Diabetologia* **52**, 1334–1338 (2009).
38. Vimaleswaran, K.S. *et al.* Physical activity attenuates the body mass index-increasing influence of genetic variation in the *FTO* gene. *Am. J. Clin. Nutr.* **90**, 425–428 (2009).

ONLINE METHODS

Gene targeting and genotyping. The targeting construct for generation of *Fto*-overexpressing mice was generated by insertion of the *Fto* complementary DNA (cDNA) into a pCAGGs-STOP-EGFP-ROSA-TV plasmid (downstream of the STOP cassette; **Supplementary Fig. 1a**). Further details are available on request. The linearized targeting vectors were electroporated into R1 embryonic stem cells[39]. Targeted embryonic stem cells were injected into C57BL/6J blastocysts to generate chimeras that transmitted the targeted allele when crossed to C57BL/6J mice. F1 mice were crossed to a line carrying the β-actin-Cre recombinase (Jackson Laboratory, stock name Tg(ACTA1-cre)79Jme/J) on a C57BL/6J background, and the offspring were backcrossed again to C57BL/6J to remove Cre recombinase. These mice were then intercrossed in multiple different matings to generate the test populations. Genotyping was performed on DNA extracted using the QIAGEN DNeasy blood and tissue kit (Qiagen) (**Supplementary Table 3**).

Animal experiments. All animal studies were carried out in accordance with UK Home Office legislation and local ethical guidelines issued by the Medical Research Council (Responsibility in the Use of Animals for Medical Research, July 1993). Mice were kept under controlled light (light 7 a.m. to 7 p.m., dark 7 p.m. to 7 a.m.), temperature (21 °C ± 2 °C) and humidity (55% ± 10%) conditions. They had free access to water (25 p.p.m. chlorine). They were fed *ad libitum* on a commercial diet (SDS Rat and Mouse No.3 Breeding diet (RM3)) containing 11.5 kcal% fat, 23.93 kcal% protein and 61.57 kcal% carbohydrate. Where indicated, mice were maintained on a high-fat diet (D12451, Research Diets) containing 45 kcal% fat, 20 kcal% protein and 35 kcal% carbohydrate. Phenotyping tests were performed according to EMPReSS (European Phenotyping Resource for Standardised Screens from EUMORPHIA) standardized protocols as described (see URLs).

RNA extraction and quantitative PCR. Total RNA was prepared from brain, hypothalamus, gastrocnemius muscle, pancreas, BAT and epigonadal WAT of free-fed female mice using the RNeasy fibrous Mini Kit, RNeasy for skeletal muscle, a Lipid Tissue Mini Kit for BAT and WAT (Qiagen), and an RNeasy Plus Mini Kit (Qiagen) for hypothalamus, according to the manufacturer's protocol. RNA concentration was assessed using a NanoDrop ND-1000 spectrophotometer (Thermo-Fischer Scientific). Extracted RNA was stored at −80 °C.

cDNA was prepared using superscript III reverse transcriptase (Invitrogen) according to the manufacturer's instructions. For each tissue, quantitative PCR was performed using TaqMan Gene Expression Assay reagents and TaqMan FAM dye–labeled probes (Applied Biosystems) using an ABIPRISM 7700 Fast Real-Time PCR System (Applied Biosystems). All data were normalized to expression of *GAPDH*, the endogenous housekeeping gene encoding glyceraldehyde 3-phosphate dehydrogenase, and analyzed by the comparative $\Delta\Delta C_T$ method to determine the difference in sample groups relative to control animals. *Hrpt* and *Egfp* were tested by semiquantitative PCR using the primers described[18,40].

Protein extraction and immunoblotting. Mouse skeletal muscle and liver tissue samples were homogenized and protein blotting was performed as described[19]. Protein blots were performed on 40 μg of total proteins using a custom rabbit anti–recombinant mFTO antibody.

Body composition analysis. Body composition was analyzed by dual-energy X-ray absorptiometry (DEXA) using the Lunar PIXImus Mouse Densitometer (Wipro, GE Healthcare).

Histology. Mice were killed by exsanguination. Epigonadal WAT was dissected and fixed in neutral buffered formaldehyde (Surgipath Europe Ltd). Paraffin-embedded sections of epigonadal WAT were stained with hematoxylin and eosin. Photomicrographs were captured by optic microscopy (Zeiss Axiostar Plus) with the ALTRA20 Soft Imaging System (Olympus). Adipocyte area was measured under the same microscope at ×40 magnification with the aid of computerized image analysis (Soft Imaging System, Olympus).

Metabolic and endocrine testing. Mice (10 weeks or 19 weeks) were placed in metabolic cages (Techniplast) for measurement of food, water and urine. Plasma leptin, insulin and adiponectin levels were measured using a mouse endocrine MILLIPLEX kit (MILLIPLEX MAP, Millipore) and a Bio-Plex 200 system (Bio-Rad) according to the manufacturer's instructions. Plasma insulin was measured at 8 weeks, 16 weeks and 20 weeks of age, and leptin was measured at 8 weeks and 20 weeks. At 20 weeks, fasted mice were anesthetized and killed by exsanguination, and blood was collected by cardiac puncture. Plasma concentrations of albumin, glucose, triglycerides, alkaline phosphatase, alanine aminotransferase, aspartate aminotransferase, free fatty acids, lactate dehydrogenase creatine kinase, total cholesterol, HDL cholesterol and LDL-cholesterol were measured on an AU400 (Olympus) as described[41].

Metabolic rate and activity measurements. Metabolic rate was measured at 18 weeks of age using indirect calorimetry (Oxymax) to determine oxygen consumption, carbon dioxide production, RER and heat production[19]. Oxygen consumption and carbon dioxide production were normalized to body weight, fat and lean tissue mass. Heat production (energy expenditure) was calculated using the equation heat = CV × VO_2, where CV = 3.815 + 1.232 × RER (CV, calorific value based on the observed respiratory exchange ratio; Oxymax, Columbus Instruments). Physical activity was assessed by circadian wheel-running activity[42].

Intraperitoneal glucose tolerance test. Mice were fasted overnight (16 h) to establish a baseline glucose level 'T_0' (time zero). Mice were weighed, and a blood sample was collected from the tail vein after administration of local anesthetic (EMLA cream, Eutectic Mixture of Local Anesthetics, Lidocaine/Prilocaine, AstraZeneca) using Lithium-Heparin microvette tubes (Sarstedt). The mice were then injected intraperitoneally with 2 g of glucose per kg body weight (20% glucose in 0.9% NaCl). Blood samples were taken at 60 min and 120 min (or 10 min, 20 min and 30 min) after injection. Plasma glucose was measured using an Analox Glucose Analyser GM9. Plasma insulin was measured using a Mercodia ultrasensitive mouse ELISA kit. AUC analysis was performed using GraphPad Prism version 5.02 for Windows.

Statistical methods. Results are expressed as mean ± s.e.m. Comparisons between two groups were made using an unpaired two-tailed Student's *t*-test and one-way analysis of variance with repeated measures, as appropriate (GraphPad Prism). AUC analysis was performed using GraphPad Prism. The relationship between body compositions, including body weight, lean mass, fat mass and FM/LM, with food intake, leptin, oxygen consumption, and carbon dioxide production were evaluated by linear regression analysis (GraphPad Prism). $P < 0.05$ was considered to be statistically significant. Multiple regression analysis was carried out using R (see URLs).

39. Nagy, A., Rossant, J., Nagy, R., Abramow-Newerly, W. & Roder, J.C. Derivation of completely cell culture-derived mice from early-passage embryonic stem cells. *Proc. Natl. Acad. Sci. USA* **90**, 8424–8428 (1993).
40. Girard, C.A. *et al.* Expression of an activating mutation in the gene encoding the KATP channel subunit Kir6.2 in mouse pancreatic beta cells recapitulates neonatal diabetes. *J. Clin. Invest.* **119**, 80–90 (2009).
41. Hough, T.A. *et al.* Novel phenotypes identified by plasma biochemical screening in the mouse. *Mamm. Genome* **13**, 595–602 (2002).
42. Bacon, Y. *et al.* Screening for novel ENU-induced rhythm, entrainment and activity mutants. *Genes Brain Behav.* **3**, 196–205 (2004).